

Published in final edited form as:

*Muscle Nerve*. 2016 April ; 53(4): 598–607. doi:10.1002/mus.24780.

## Magnetic stimulation supports muscle and nerve regeneration after trauma in mice

Meline N. L. Stölting, MD, PhD<sup>1</sup>, Anne Sophie Arnold, PhD<sup>2</sup>, Deana Haralampieva, M.Sc.<sup>1</sup>, Christoph Handschin, PhD<sup>2</sup>, Tullio Sulser, Prof.<sup>1</sup>, and Daniel Eberli, MD, PhD<sup>1,\*</sup>

<sup>1</sup>Laboratory for Urologic Tissue Engineering and Stem Cell Therapy, Division of Urology, University of Zurich, Frauenklinikstrasse 10, CH 8091 Zurich, Switzerland <sup>2</sup>Biozentrum, Focal Area Growth and Development, University of Basel, Klingelbergstrasse 50-70, CH-4056 Basel, Switzerland

### Abstract

**Introduction**—Magnetic stimulation (MS) has the ability to induce muscle twitch and has long been proposed as a therapeutic modality for skeletal muscle diseases. However, the molecular mechanisms underlying its means of action have not been defined.

**Methods**—Muscle regeneration after trauma was studied in a standard muscle injury mouse model. The influence of MS on the formation of motor-units, post-trauma muscle/nerve regeneration, and vascularization was investigated.

**Results**—We found that MS does not cause systemic or muscle damage but improves muscle regeneration by significantly minimizing the presence of inflammatory infiltrate and formation of scars after trauma. It avoids post-trauma muscle atrophy, induces muscle hypertrophy, and increases the metabolism and turnover of muscle. It triples the expression of muscle markers and significantly improves muscle functional recovery after trauma.

**Discussion**—Our results indicate that MS supports muscle and nerve regeneration by activating muscle-nerve cross-talk and inducing the maturation of NMJs.

### Keywords

Magnetic Stimulation Therapy; Nerve Regeneration; Rehabilitation Outcome; Muscle Contraction; Neuromuscular Junction

---

\*Corresponding Author: Daniel.Eberli@usz.ch, Phone: +41 44 255 9619, Fax: +41 44 255 9620.

**Declaration of Conflicting Interests:** The authors declare no conflicts of interest with respect to the authorship and/or publication of this article.

#### Reprint request

Unfortunately, due to copyright-related issues, we are not able to post the post-print pdf version of our manuscript - in some cases, not even any version of our manuscript. Thus, if you would like to request a post-production, publisher pdf reprint, please click send an email with the request to christoph-dot-handschin\_at\_unibas-dot-ch (see <http://www.biozentrum.unibas.ch/handschin>).

Information about the Open Access policy of different publishers/journals can be found on the SHERPA/ROMEO webpage: <http://www.sherpa.ac.uk/romeo/>

## Introduction

Magnetic stimulation (MS) was originally developed to stimulate central and peripheral nerves 1,2. More recently it has been proposed to promote neuromodulation and exercise training of deficient skeletal muscle 3,4. In humans, a magnetic coil wrapped around the quadriceps has been demonstrated to induce effortless muscle fatigue and training 4,5. A similar device for exercising the pelvic floor was designed in which magnetic pulses converged into a coil placed inside a chair seat 6. Magnetic stimulation has been used to treat urinary incontinence in women 7,8. Although promising preliminary clinical reports have been published 9,10, contradictory clinical studies with opposing outcomes using central 11,12 and peripheral MS 13 treatments urged the necessity for investigations demonstrating if and how MS could support the cellular machinery of muscle and/or nerves to promote muscle training 8.

Nerve repair and prevention of post-traumatic muscle atrophy represent a major challenge in medical care. After trauma, an initial cleanup of damaged structures is necessary before natural reconstruction can take place. Schwann cells are the main cells responsible for removing damaged myelin, while macrophage infiltration is necessary for breakdown of damaged fragments of cells and fibers 14. Meanwhile, in the midst of the inflammatory reaction, muscle satellite cells are activated for muscle reconstruction. During this process, they fuse and build new myofibers with central nuclei, allowing muscle regeneration to occur within weeks 15. The newly formed myofibers require rapid functional innervation and mature neuromuscular junctions (NMJs) to complete their differentiation process and recover strength 16. Exercise is known to improve posttraumatic peripheral nerve lesions and improve function. MS can produce stimuli equivalent to endurance exercise in humans 4, but the mechanisms by which this occurs, as well as its impact on post-traumatic muscle reconstruction, remain poorly understood.

In this study, a mouse muscle crush injury model was used to investigate the mode of action of MS on muscle tissue stimulation and post-trauma regeneration. The formation of motor units by MS was evaluated by assessing the clustering of acetylcholine receptors (AChRs) and known muscular metabolic adaptations caused by muscle contraction. Here, the influence of MS on post-trauma muscle/nerve regeneration and vascularization is investigated in detail, and its overall systemic impact is discussed.

## Materials and Methods

### Ethical and animal experimental approval

The animal experiments described in this study were analyzed carefully and approved by the Swiss veterinary inspection office of the canton of Zurich. The Swiss guidelines on animal welfare were followed rigorously. To assure minimum discomfort for the animals, a single intervention with crush injury and intramuscular injection of cells was performed, followed by muscle training under anesthesia.

## Muscle injury and magnetic stimulation *in vivo*

Upon ethical and animal experimental approval 48 C57 mice (3-month-old females) received an upper-leg lateral incision from the lateral knee to the greater trochanter while under 5% isoflurane anesthesia using aseptic conditions, including shaved skin and betadine asepsis 17. A coronal plane was opened beneath the quadriceps, separating the muscle from the femur. The lower jaw of an artery forceps 18 was inserted gently below the quadriceps. The crush injury was performed by closing the forceps to their first stage for 5 seconds, which produced a reproducible transverse injury of about 4mm. The forceps was gently removed, and the wound was closed.

The animals were allowed free cage activity and free access to food and water. The animals received Carprofen (5 mg/kg/KGW, SC) prior to muscle injury, every 12 h thereafter, and at any sign of distress. After 5 days, the animals were divided randomly into 2 groups. Twenty mice received 3 sessions of 20 minutes MS under anesthesia (2.00 mg/30 g Ketamine and 0.06 mg/30 g Azepromazine) every second day delivered by the Biocon-2000W™ (Mcube Technology Co Ltd, Korea). The Biocon 2000W has a CE certification for clinical use (CE 120) and is sold in Europe and Asia. The manufacturer specifies a maximal electric power consumption of 2.5 kVA with a maximal discharge voltage of 1800V and a maximal two-phase discharge current of 2200A at the level of the coil. The thighs of the animals were placed at the center of the coil, and each MS session was performed as described previously 6 (10 min/10Hz and 10min/50 Hz, each pulse consisting of 3 s stimulation, 6 s rest). The other 20 mice with crush injuries served as controls. In order to rule out the effect of the anesthesia on muscle regeneration, control animals underwent anesthesia but received no MS. To assess the effect of MS in the absence of trauma, the remaining 8 mice received no muscle injury, and half of them were submitted to MS. Euthanasia was performed using CO<sub>2</sub> followed by exsanguination.

## Immunohistochemistry

The tissues were harvested 5 days after MS therapy to evaluate muscle regeneration, muscle atrophy, myofiber typing, and NMJ formation, as previously described 19. Briefly, the quadriceps muscle was removed, minced, and incubated in 0.2% collagenase (60 min, 37 °C). Single muscle fibers were liberated by shearing using heat-polished Pasteur pipettes, washed in PBS and fixed (4% paraformaldehyde, 10 min). Then, they were incubated in 0.3 M glycine (20 min), stained with  $\alpha$ -BTX (1:20, Invitrogen) and DAPI (1:100, Sigma) for 1 hour, washed twice in PBS, transferred to a glass slide in DABCO (Sigma), and analyzed by fluorescence microscopy. At a 63 $\times$  magnification, 20 fields were chosen randomly, and the number of NMJs was counted. The relative number of AChR clusters per muscle fiber (50 muscle fibers per group) was analyzed.

For histological analyses, the quadriceps muscles were dissected, embedded in OCT, and 10- $\mu$ m frozen sections were prepared and air dried. Hematoxylin/eosin staining was carried out as described previously to assess the width of the scar and infiltration of inflammatory cells 20. Lymphocytes, neutrophils, and macrophages were not differentiated in this analysis. The tissues were fixed (100% methanol, -20 C), permeabilized (0.5% Triton X-100, 7 min), and blocked (1% BSA, 0.1% Triton X-100 in PBS, RT, 30 min). The concentrations of the

antibodies used for immunolabeling were as follows: anti-Desmin (1:100, BD Biosciences), anti-myosin-heavy-chain (1:2, DSHB, Yowa), anti-myosin-heavy-chain-slow-twitch (1:5, DSHB, Yowa), anti-myosin-heavy-fast-twitch (1:2, DSHB, Yowa), alpha-bungarotoxin (1:20, Invitrogen), antineurofilament68 (1:300, Sigma), anti-von-Willebrand-factor (1:50, Abcam), and antismoothelin (1:100, Santa Cruz). The secondary antibodies were Alexa Fluor 488 antimouse-IgG (1:100, Brunschwig), FITC-anti-mouse-IgM (1:100, Sigma), Cy3-antimouse-IgG (1:1000, Sigma), Cy3-anti-rabbit-IgG (1:100, Sigma), FITC-anti-Sheep IgG (1:100, Abcam), and DAPI (Sigma). The images were acquired at exposures that were based on unstained controls and were taken with a confocal microscope (Leica SP5, Germany).

### Histomorphometrical measurements

Muscle regeneration was evaluated by counting fibers with centrally located nuclei in 20 randomly chosen sections in a blinded fashion. This value was normalized to the total number of muscle fibers per field, which was defined as the regeneration ratio 21. Inflammatory infiltration was determined by the distance from the border of the injury that the inflammatory cells had migrated. The percentage of slow-twitch and fast-twitch fibers was determined by the immunostaining of type I fibers (FITC stained) and type II fibers (Cy3 stained). Muscle atrophy was assessed by measuring the crosssectional areas of the muscle fibers 22. Native and non-stimulated quadriceps muscles were used as controls for histology. The entire quadriceps muscle cross-section was analyzed (n=20, 20x HPF), with care taken to ensure comparable cross-section locations within and at the border of the induced muscle injury. Image J software (NIH, Bethesda, MD) for microscopy was used for measurements, and all data are expressed as the mean/SD.

### Serum creatinine, creatine kinase, bilirubin, myoglobin, and haptoglobin measurements

To evaluate possible systemic effects of MS, blood was collected in heparincoated collection tubes (BD, Biosciences), and serum was isolated by centrifugation. Serum creatinine, creatine kinase, bilirubin, myoglobin, and haptoglobin activity were then determined with specific assays kits according to the manufacturer's protocol (Diagnostic Chemicals Limited).

### Western blotting

The samples of the crushed zone were carefully dissected, and western blot (WB) was performed as previously described 20. In summary, the tissues were pulverized in liquid nitrogen with a mortar and pestle, washed with PBS/protease inhibitor cocktail (P8340, Sigma), and lysed. The protein lysates were measured using the Pierce BCA Protein Assay Kit (Thermo Scientific), loaded on 12% Bio-Rad gels (30 µg), transferred onto PVDF membranes (Immobilon-P; Millipore, Bedford, MA), blocked 1 h in 5% non-fat dry milk, and incubated overnight at 4 °C with the primary antibodies. The primary antibodies were mouse anti-Desmin (1:500, BD Biosciences), mouse anti-myosin-heavy-chain (1:50, DSHB, Yowa), mouse anti-myosin-heavy-chain I (1:25, DSHB, Yowa), mouse anti-myosin-heavy-chain II (1:25, DSHB, Yowa), mouse PGP9.5-Neuronal Marker (1:2000, Abcam), anti-neurofilament 68 (1:1000, Sigma), rabbit anti-Agrin (1:200, Santa Cruz), and monoclonal anti-GAPDH (1:2000, Sigma). The membranes were washed in TBS/0.1% Tween-20 (30 min) and incubated for 1 h with the appropriate HRP-conjugated secondary antibody

(Amersham, Dubendorf, Switzerland) in TBS/0.1% Tween-20/5% non-fat dry milk. The membranes were developed using the ECL technique (ECL-Kit, Amersham, Freiburg, Germany). The protein amounts were normalized to GAPDH. The quantification of each protein was performed using Image J software (NIH, Bethesda, MD).

## Myography

After careful dissection, muscle strips were kept under tension with constant oxygenation (95% O<sub>2</sub> and 5% CO<sub>2</sub>) in Krebs solution at room temperature. Muscle strips were fastened with vicryl into the myograph-chambers (DMT, Denmark) and allowed to equilibrate for 20 min under 20 mN tension at 37 °C. Every 5 minutes, the tension was adjusted, and the Krebs solution was replaced. Single 80 V/80 Hz twitch stimulations were used to determine the optimum length (L<sub>0</sub>) of each tissue, and the maximum tension during tetanic contractions was registered. All data were collected using a LabChart v7.0 (ADInstruments, Spechbach, Germany) and expressed as the mean/SD.

## Statistics

All of the data are expressed as averages with their corresponding standard deviations. For statistical analysis, SPSS v11 (SPSS Inc., Chicago, IL) was used, and the graphics were drawn with GraphPad Prism v5.04 (GraphPad Software, Inc.). All data were analyzed by independent samples *t*-tests or one-way ANOVA with Bonferroni *post hoc* analysis. *P*<0.05 was considered significant.

## Results

### Magnetic stimulation causes no systemic or muscle damage but improves muscle regeneration

After 5 days of MS treatment, muscle and blood samples were collected and compared to non-stimulated controls (Figure 1). To evaluate the systemic effects of MS *in vivo*, the circulating blood concentrations of creatinine, creatine kinase, bilirubin, myoglobin, and haptoglobin were measured. During stimulation, MS triggered clearly visible muscle contractions. The levels of haptoglobin, bilirubin, and creatinine were within the normal range, indicating the absence of hemolysis and hepatic or kidney damage in both groups. Circulating myoglobin levels (Figure 1C) were similar and slightly elevated in both stimulated and control animals (24.6±2.3 µg/l and 25.2±1.3 µg/l, respectively, *P*=0.313). Conversely, the levels of creatine kinase increased 5-fold in the samples from the stimulated group (control 193.5±90.36 U/l and 933.3±10.54 U/l, respectively, *P*<0.001). This finding, associated with the comparable myoglobin levels, indicates the presence of exercise without significant additional muscle damage after MS (Figure 1D).

The histomorphometrical analysis of the muscle injury site (Figures 1E, 1F, and 1G) demonstrated that the MS-treated group showed a reduction in post-traumatic scar formation (214.2±57.8 µm) equal to one-third of the control values (686.3±71.8 µm, *P*<0.001). The samples from the MS group also demonstrated reduced infiltration of inflammatory cells (347.4±18.9 µm), while samples from the control group displayed inflammatory cells at distances of up to 637.5±64.02 µm of the scar interface (*P*<0.001). In addition, we assessed

the presence of neovascularization by comparing the double-staining of von Willebrand factor (vWf) and smoothelin in both groups (Figures 1I and 1J). As expected, the injury site of the non-stimulated samples had increased vascularization (vWf  $162 \pm 19.2\%$ ,  $P=0.003$  and smoothelin  $190.8 \pm 24.4\%$ ,  $P=0.001$ ). However, in the MS-treated samples, the number of vessels within the scar was reduced to values similar to that of unscathed control muscle 5 days after injury (vWf  $96.3 \pm 6.3\%$  and smoothelin  $97.9 \pm 25.0\%$ ).

### **Magnetic stimulation reduces post-trauma muscle atrophy and induces the hypertrophy of unscathed tissue**

Muscle fiber cross-section measurements were performed within the injury region and at the interface with normal muscle (Figure 2). We found that the myofibers within the injury regions without MS had reduced cross-sections of  $38.56\% \pm 1.64$  ( $P<0.001$ , Figures 2A, 2B, and 2C) of an intact quadriceps myofiber. In contrast, MS-stimulated muscle did not undergo atrophy, showing fiber cross-section values similar to or larger than unharmed non-stimulated controls ( $114.4\% \pm 5.2$ ,  $P<0.05$ ). Furthermore, the muscle regenerative process, demonstrated by the presence of myotubes with central nuclei, was significantly increased ( $P<0.001$ ) by MS (Figure 2D). A total of  $80.7\% \pm 7.0$  of the muscle fibers in the injury site of MS-treated samples displayed central nuclei, whereas only  $41.5\% \pm 8.1$  of myofibers in untreated crushed muscle fibers were regenerating myofibers.

Additional analyses of tissue at the injury interface demonstrated that the muscle adjacent to the trauma location became atrophic in non-stimulated samples. Specifically, the muscle fiber cross-sections were reduced to  $69.9 \pm 8.5\%$  of control ( $P=0.002$ , Figures 2E, 2F, and 2G). MS treatment was sufficient to prevent this process, not only by inducing hypertrophy ( $134.5 \pm 6.5\%$ ,  $P<0.001$ ) but also by again increasing the regenerative process (Figures 2G and 2H). At the interface with normal muscle, we found that  $50.0 \pm 7.2\%$  of the MS-treated myofibers displayed central nuclei, while only  $20.1 \pm 2.0\%$  of the untreated sample myofibers were regenerating (Figure 2H).

### **Magnetic stimulation induced a shift of muscle fiber type to slow-twitch and improved muscle contractile force**

Analyses of immunostained muscle slices and semi-quantitative protein measurements were performed to estimate the impact of MS on muscle protein expression and fiber typing. Muscle-specific proteins, such as myosin heavy chain (MyH), tended to increase (control  $0.43 \pm 0.06$ , stimulated  $0.74 \pm 0.26$ ,  $P=0.056$ ), and desmin (Figure 3A) doubled its expression after 5 days of magnetic stimulation (control  $0.78 \pm 0.25$ , stimulated  $1.6 \pm 0.26$ ,  $P=0.021$ ). Our western blot (WB) results indicated a 3-fold increase in MyH1 (control  $0.42 \pm 0.11$  and stimulated  $1.46 \pm 0.31$ ,  $P<0.001$ , Figure 3B), whereas no significant increase in MyH2 expression (control  $0.11 \pm 0.10$  and stimulated  $0.19 \pm 0.07$ ,  $p=0.09$ , Figure 3C) could be detected after stimulation.

Immunostaining with MyH1/MyH2 confirmed the WB data, demonstrating that MS boosted MyH type 1 expression (Figures 3D and 3E) when compared to non-stimulated controls ( $128.3 \pm 24.4\%$ ,  $P<0.05$ ) and native control quadriceps ( $278.8 \pm 35.6\%$ ,  $P<0.001$ , Figure 3F). When compared to native control muscle tissue, the consequent decrease in MyH type 2



(control  $103.4 \pm 13.4\%$ ,  $P=0.2643$  and stimulated  $68.6 \pm 9.3\%$ ,  $P<0.001$ ) after MS (Figure 3G) again underlined the shift to slow-twitch fibers.

The myography of native control and damaged muscle tissue demonstrated that MS improved the contractile force of normal muscle and supported the recovery of muscle contractile response to electrical stimulation after damage (Figure 4). In the absence of trauma, muscle tetanic contraction forces significantly increased after 5 days of training with MS, as demonstrated in 2 electrical stimulation settings: 40 V/40 Hz (control  $3.34 \pm 0.7$  g and stimulated  $5.7 \pm 1.2$  g,  $P<0.05$ ) and 80 V/80 Hz (control  $8.0 \pm 1.3$  g and stimulated  $13.7 \pm 2.7$  g,  $P<0.05$ , Figure 4A). As demonstrated in Figure 4B, crush injury was sufficient to reduce muscle strength to approximately one-half of native controls (crush injury  $4.6 \pm 1.0$  g and native controls  $9.4 \pm 3.2$  g). Likewise, a significant recovery of muscle strength could be observed following crush injury after 5 days of treatment with MS using 40 V/40 Hz (control  $1.03 \pm 0.27$  g and stimulated  $2.5 \pm 0.2$  g,  $P<0.001$ ) and 80 V/80 Hz (control  $2.6 \pm 0.9$  g and stimulated  $4.7 \pm 0.5$  g,  $P<0.05$ , Figure 4C). This recovery was sufficient to recover muscle strength values comparable to uninjured muscle (control  $3.3 \pm 0.7$  g and stimulated  $2.5 \pm 0.2$  g,  $P=0.216$ , Figure 4D), suggesting that MS may be useful for muscle rehabilitation after trauma.

### **Magnetic stimulation promotes nerve ingrowth and acetylcholine receptor clustering after injury**

To verify the influence of MS in recovery of innervation after injury, we analyzed the regenerating muscle tissue by evaluating muscle/nerve components and the formation of NMJs. We found evidence of improved cross-talk between muscles and nerves (Figure 5A), thus promoting the maturation of neuromuscular junctions (NMJs) after MS treatment. Agrin levels were significantly higher in MS-treated samples (control  $0.70 \pm 0.17$  and treated  $1.06 \pm 0.13$ ,  $P=0.046$ ). Likewise, expression of neurofilament protein NF68 (control  $0.71 \pm 0.10$  and treated  $1.26 \pm 0.16$ ,  $P=0.026$ ) and PGP 9.5 (control  $0.47 \pm 0.12$  and treated  $0.78 \pm 0.15$ ,  $P=0.003$ ) were upregulated (Figures 5B and 5C). Additionally, the coefficient of the stimulated samples was not only higher than that of non-stimulated samples (control  $40.7 \pm 4.0$  and stimulated  $143.9 \pm 21.7$ ,  $P<0.001$ ) but also surpassed ( $P=0.036$ ) even the coefficient found in a normal quadriceps muscle (Figures 5D, 5E, and 5F). Moreover, the total number of AChR clusters per high-power field (HPF) was clearly higher in MS-treated samples (control  $3.9 \pm 0.6$  and treated  $7.1 \pm 1.1$ ,  $P=0.021$ , Figures 5G, 5H, and 5I). Finally, AChR displayed better organization and distribution in the MS-treated muscle fibers (control  $0.07 \pm 0.04$  and treated  $0.61 \pm 0.09$ ,  $P<0.001$ ), with up to 8-fold increases in the total number of clusters per muscle fiber (Figures 5J, 5K, and 5L).

### **Discussion**

Magnetic fields can be used to trigger muscle contraction. However, clinical studies remain inconclusive, and no molecular mechanism underlying this action has been described. Using an *in vivo* model of muscle injury, we studied the impact of MS treatment on post-traumatic muscle and nerve regeneration. We found that MS a) causes no systemic or muscle damage; b) improves muscle regeneration by reducing inflammatory infiltrate and avoiding post-

trauma muscle atrophy; c) improves muscle contractile function by inducing myofiber hypertrophy; d) promotes acetylcholine receptor clustering and nerve ingrowth after injury; and in our setting, e) induces a muscle fiber type switch to slow-twitch.

The major advantage that makes MS an interesting rehabilitation treatment modality is its capability to excite a specific target in a painless and non-invasive manner. In our mouse model, we found that only creatine kinase (CK) levels increased, which, in the absence of other rhabdomyolysis markers, indicates a muscle workout without significant tissue damage 23. After endurance exercise, CK is expected to increase at least 3-fold compared to resting conditions 24. Earlier studies have supported our findings by establishing that MS causes less damage to muscle than direct electrical stimulation, as indicated by only a limited rise of creatine metabolites 25. MS has also been used in patients with chronic illness, including chronic obstructive pulmonary disease (COPD) 4, multiple sclerosis, 26 and hypertension, 27 and even during pregnancy 28 without complications.

MS could play an important role in post-traumatic skeletal muscle regeneration. A previous report has suggested that MS might facilitate regeneration in skeletal muscle damage induced by mepivacaine 29. However, this anesthetic is known to produce muscle fiber lysis while sparing the vascular bed, nerve endings, and satellite cells 30 and is therefore not a good model for the damage caused by trauma. In our experiments we excluded the effects of anesthesia on muscle regeneration by exposing all animals (treated or controls) to the same number of anesthesia sessions. We have demonstrated the post-trauma impact of MS treatment in promoting muscle regeneration, nerve ingrowth, and AChR clustering in a mouse model after muscle crush. MS decreased the inflammatory infiltrate, prevented myofiber atrophy, boosted muscle protein expression, and significantly increased the number of regenerating fibers.

We observed that MS influences native muscle fibers adjacent to the site of injury, inducing phenotypic changes compatible with the effects of exercise. MS increased fiber cross-section and even supported new fiber formation within healthy regions of the muscle. We also found that repetitive muscle stimulation for 20 minutes every second day during muscle healing can significantly support regeneration. Recent studies have demonstrated that magnetic fields induce myoblast differentiation 31 and promote myofiber hypertrophy 32. The increased number of myofibers with central nuclei at the injury interface of MS-stimulated samples seems to play an important role in the overall regeneration process of the damaged tissue. This finding, together with the hypertrophic state of MS-treated muscles, would explain the decrease in size of the injury scar in stimulated samples. We speculate that MS has the potential to activate and induce differentiation of resident satellite cells *in situ*. This is important, because it indicates that MS acts not only at sites of injury but also in adjacent tissues, which could then synergistically improve regeneration and muscle rehabilitation after trauma. Early NMJ formation is marked by intensive cross-talk between muscle cells and nerve fibers that is mediated through Agrin secretion. Agrin is a heparan sulfate proteoglycan that activates muscle-specific kinase (MuSK) to cluster cholinergic receptors in the post-synaptic endplate 33. It also acts as an envoy between the nerves and muscles, initiating the cascade that promotes NMJ maturation and regulates synaptic function 34. Our results indicate that the increase in neuronal ingrowth detected in MS-treated tissues was



also associated with an increase in Agrin. This finding went hand-in-hand with muscle differentiation and accumulation of AChR, which is known to indicate a functional NMJ 35. Finally, our results indicate that in the settings used, MS mimics the effects of exercise, which increases turnover and causes hypertrophy in skeletal muscle 36. Taken together, these findings indicate that MS induces neuronal ingrowth and myoblast differentiation by promoting muscle-nerve cross-talk and inducing the maturation of NMJs.

With the settings used, MS distinctly influenced muscle fiber type-decision. We found that during the regeneration process *in vivo*, fibers formed under MS treatment tended to shift their fiber type to slow-twitch (MyH1). It has been described that during regeneration, newly formed myotubes tend to follow the intrinsic typing characteristics of the prior fibers 37. Although the quadriceps is mainly a fast-twitch type of muscle 38, we detected a 3-fold increase in type 1 (slow-twitch) fibers after MS treatment. These results propose that MS could be an efficient support to post-trauma rehabilitation after acute nerve and muscle damage. Astonishingly, these results were achieved in mice after as few as 3 sessions of 20 minutes of MS (10 min/10Hz followed by 10min/50 Hz). The device used in this study has been developed to treat stress urinary incontinence in humans and is designed to reach the human pelvic floor in the sitting position. We acknowledge that this is beyond what would be necessary to stimulate the lower legs of a small C57 mouse alone. This study cannot answer if a lower magnitude of stimulation would induce similar results. Further, systematic studies exploring the effects of MS on functional rehabilitation in chronically damaged skeletal muscle would complete our understanding of the mechanisms by which MS acts on muscle injury.

## Acknowledgments

We gratefully acknowledge the technical assistance of Dr. Souzan Salemi and Fatma Kivrak with the improvement of our FACS, IHC and WB methods. This work was supported by the Hartmann-Muller Foundation, Forschungskredit, Swiss National Foundation and the University of Zurich.

**Funding:** The authors disclose receipt of the following sources of financial support for the research and/or authorship of this article: Swiss National Foundation and University of Zurich.

## Abbreviations

<b><math>\alpha</math>-BTX</b>	$\alpha$ -bungarotoxin
<b>AChRs</b>	acetylcholine receptors
<b>CK</b>	creatine kinase
<b>HPF</b>	high-power-field
<b>MS</b>	magnetic stimulation
<b>MuSK</b>	muscle-specific kinase
<b>MyH</b>	myosin heavy chain
<b>NMJ</b>	neuromuscular junction

<b>vWf</b>	Willebrand factor
<b>WB</b>	western blot

## References

1. Barker AT, Jalinous R, Freeston IL. Non-invasive magnetic stimulation of human motor cortex. *The Lancet*. 1985; 325(8437):1106–1107.
2. Bickford RG, Guidi M, Fortesque P, Swenson M. Magnetic stimulation of human peripheral nerve and brain: response enhancement by combined magneto-electrical technique. *Neurosurgery*. 1987; 20(1):110–116. [PubMed: 3808250]
3. Polkey MI, Luo Y, Guleria R, ARd C-HH, Green M, Moxham J. Functional Magnetic Stimulation of the Abdominal Muscles in Humans. *American Journal of Respiratory and Critical Care Medicine*. 1999; 160(2):513–522. [PubMed: 10430722]
4. Swallow EB, Gosker HR, Ward KA, et al. A novel technique for nonvolitional assessment of quadriceps muscle endurance in humans. *Journal of Applied Physiology*. 2007; 103(3):739–746. [PubMed: 17569771]
5. Taylor JL. Magnetic muscle stimulation produces fatigue without effort. *Journal of Applied Physiology*. 2007; 103(3):733–734. [PubMed: 17600156]
6. Chandi DD, Groenendijk PM, Venema PL. Functional extracorporeal magnetic stimulation as a treatment for female urinary incontinence: 'the chair'. *BJU International*. 2004; 93(4):539–542. [PubMed: 15008725]
7. Quek P. A critical review on magnetic stimulation: what is its role in the management of pelvic floor disorders? *Current Opinion in Urology*. 2005; 15(4):231–235. [PubMed: 15928511]
8. Voorham Van Der Zalm PJ, Pelger RC, Stiggelbout AM, Elzevier HW, Lycklama A Nijeholt GA. Effects of magnetic stimulation in the treatment of pelvic floor dysfunction. *BJU International*. 2006; 97(5):1035–1038. [PubMed: 16643487]
9. Hoscan MB, Dilmen C, Perk H, et al. Extracorporeal Magnetic Innervation for the Treatment of Stress Urinary Incontinence: Results of Two-Year Follow-Up. *Urologia Internationalis*. 2008; 81(2):167–172. [PubMed: 18758214]
10. Choe J, Choo M-S, Lee K-S. Symptom change in women with overactive bladder after extracorporeal magnetic stimulation: a prospective trial. *International Urogynecology Journal*. 2007; 18(8):875–880.
11. Mitchell WK, Baker MR, Baker SN. Muscle responses to transcranial stimulation in man depend on background oscillatory activity. *The Journal of Physiology*. 2007; 583(2):567–579. [PubMed: 17627997]
12. Ellaway PH, Davey NJ, Maskill DW, Rawlinson SR, Lewis HS, Anissimova NP. Variability in the amplitude of skeletal muscle responses to magnetic stimulation of the motor cortex in man. *Electroencephalography and clinical Neurophysiology*. 1998; 109:104–113. [PubMed: 9741800]
13. Wallis MC, Davies EA, Thalib L, Griffiths S. Pelvic Static Magnetic Stimulation to Control Urinary Incontinence in Older Women: A Randomized Controlled Trial. *Clinical Medicine & Research*. 2012; 10(1):7–14. [PubMed: 21817123]
14. Sarikcioglu L, Yaba A, Tanriover G, Demirtop A, Demir N, Ozkan O. Effect of Severe Crush Injury on Axonal Regeneration: A Functional and Ultrastructural Study. *J reconstr Microsurg*. 2007; 23(03):143–149. [PubMed: 17479452]
15. Charge SBP, Rudnicki MA. Cellular and Molecular Regulation of Muscle Regeneration. *Physiological Reviews*. 2004; 84(1):209–238. [PubMed: 14715915]
16. Lin S, Landmann L, Ruegg MA, Brenner HR. The Role of Nerve- versus Muscle-Derived Factors in Mammalian Neuromuscular Junction Formation. *J Neurosci*. 2008; 28(13):3333–3340. [PubMed: 18367600]
17. Bunn, Jonathan R.; C, J.; Burke, George; Mushipe, Moses; Marsh, David R.; Li, Gang. Production of consistent crush lesions in murine quadriceps muscle - A biomechanical, histomorphological and immunohistochemical study. *Journal of Orthopaedic Research*. 2004; 22(6):1336–1344. [PubMed: 15475218]

18. Collins RA, Grounds MD. The Role of Tumor Necrosis Factor- $\alpha$  (TNF- $\alpha$ ) in Skeletal Muscle Regeneration: Studies in TNF- $\alpha$ (-/-) and TNF- $\alpha$ (-/-)/LT- $\alpha$ (-/-) Mice. *J Histochem Cytochem*. 2001; 49(8):989–1002. [PubMed: 11457927]
19. Handschin C, Kobayashi YM, Chin S, Seale P, Campbell KP, Spiegelman BM. PGC-1 $\alpha$  regulates the neuromuscular junction program and ameliorates Duchenne muscular dystrophy. *Genes & Development*. 2007; 21(7):770–783. [PubMed: 17403779]
20. Stölting MNL, Ferrari S, Handschin C, et al. Myoblasts Inhibit Prostate Cancer Growth by Paracrine Secretion of Tumor Necrosis Factor- $\alpha$ . *J Urol*. 2013; 189(5):1952–1959. [PubMed: 23123370]
21. Sandri M, Sandri C, Gilbert A, et al. Foxo Transcription Factors Induce the Atrophy-Related Ubiquitin Ligase Atrogin-1 and Cause Skeletal Muscle Atrophy. *Cell*. 2004; 117(3):399–412. [PubMed: 15109499]
22. Sandri M, Jiandie, Handschin Christoph, Yang Wenli, Arany Zoltan P, Lecker Stewart H, Goldberg Alfred L, Spiegelman Bruce M. PGC-1  $\alpha$  protects skeletal muscle from atrophy by suppressing FoxO3 action and atrophy-specific gene transcription. *Proceedings of the National Academy of Sciences*. 2006; 103(44):16260–16265.
23. Ross JH, Attwood EC, Atkin GE, Villar RN. A study on the effects of severe repetitive exercise on serum myoglobin, creatine kinase, transaminases and lactate dehydrogenase. *Q J Med*. 1983; 52(206):268–279. [PubMed: 6611841]
24. Totsuka M, Nakaji S, Suzuki K, Sugawara K, Sato K. Break point of serum creatine kinase release after endurance exercise. *Journal of Applied Physiology*. 2002; 93(4):1280–1286. [PubMed: 12235026]
25. Chiba A, Inase M. Phosphate metabolites in muscular contraction caused by magnetic stimulation. *Bioelectromagnetics*. 2003; 24(5):366–371. [PubMed: 12820294]
26. de Carvalho MLL, Motta R, Konrad G, Battaglia MA, Brichetto G. A randomized placebo-controlled cross-over study using a low frequency magnetic field in the treatment of fatigue in multiple sclerosis. *Multiple Sclerosis Journal*. 2012; 18(1):82–89. [PubMed: 21788248]
27. Cogiamanian F, Brunoni AR, Boggio PS, Fregni F, Ciocca M, Priori A. Non-invasive brain stimulation for the management of arterial hypertension. *Medical Hypotheses*. 2010; 74(2):332–336. [PubMed: 19775822]
28. Zhang D, Hu Z. RTMS may be a good choice for pregnant women with depression. *Archives of Women's Mental Health*. 2009; 12(3):189–190.
29. Jimena I, Tasset I, Lopez-Martos R, et al. Effects of Magnetic Stimulation on Oxidative Stress and Skeletal Muscle Regeneration Induced by Mepivacaine in Rat. *Medicinal Chemistry*. 2009; 5(1): 44–49. [PubMed: 19149649]
30. Okland S, Komorowski TE, Carlson BM. Ultrastructure of mepivacaine-induced damage and regeneration in rat extraocular muscle. *Investigative Ophthalmology & Visual Science*. 1989; 30(7):1643–1651. [PubMed: 2745004]
31. Stern-Straeter J, Bonaterra GA, Kassner SS, et al. Impact of static magnetic fields on human myoblast cell cultures. *International Journal of Molecular Medicine*. 2011; 28(6):907–917. [PubMed: 21837362]
32. Coletti D, Teodori L, Albertini MC, et al. Static magnetic fields enhance skeletal muscle differentiation in vitro by improving myoblast alignment. *Cytometry Part A*. 2007; 71A(10):846–856.
33. Lin W, Burgess RW, Dominguez B, Pfaff SL, Sanes JR, Lee K-F. Distinct roles of nerve and muscle in postsynaptic differentiation of the neuromuscular synapse. *Nature*. 2001; 410(6832): 1057–1064. [PubMed: 11323662]
34. Daniels MP. The role of agrin in synaptic development, plasticity and signaling in the central nervous system. *Neurochem Int*. 2012; 61(6):848–853. [PubMed: 22414531]
35. Anglister L. Acetylcholinesterase from the motor nerve terminal accumulates on the synaptic basal lamina of the myofiber. *The Journal of Cell Biology*. 1991; 115(3):755–764. [PubMed: 1918162]
36. Burd NA, Tang JE, Moore DR, Phillips SM. Exercise training and protein metabolism: influences of contraction, protein intake, and sex-based differences. *Journal of Applied Physiology*. 2009; 106(5):1692–1701. [PubMed: 19036897]

37. Kalhovde JM, Jerkovic R, Sefland I, et al. 'Fast' and 'slow' muscle fibres in hindlimb muscles of adult rats regenerate from intrinsically different satellite cells. *The Journal of Physiology*. 2005; 562(3):847–857. [PubMed: 15564285]
38. Wang XN, Williams TJ, McKenna MJ, et al. Skeletal muscle oxidative capacity, fiber type, and metabolites after lung transplantation. *Am J Respir Crit Care Med*. 1999; 160(1):57–63. [PubMed: 10390380]

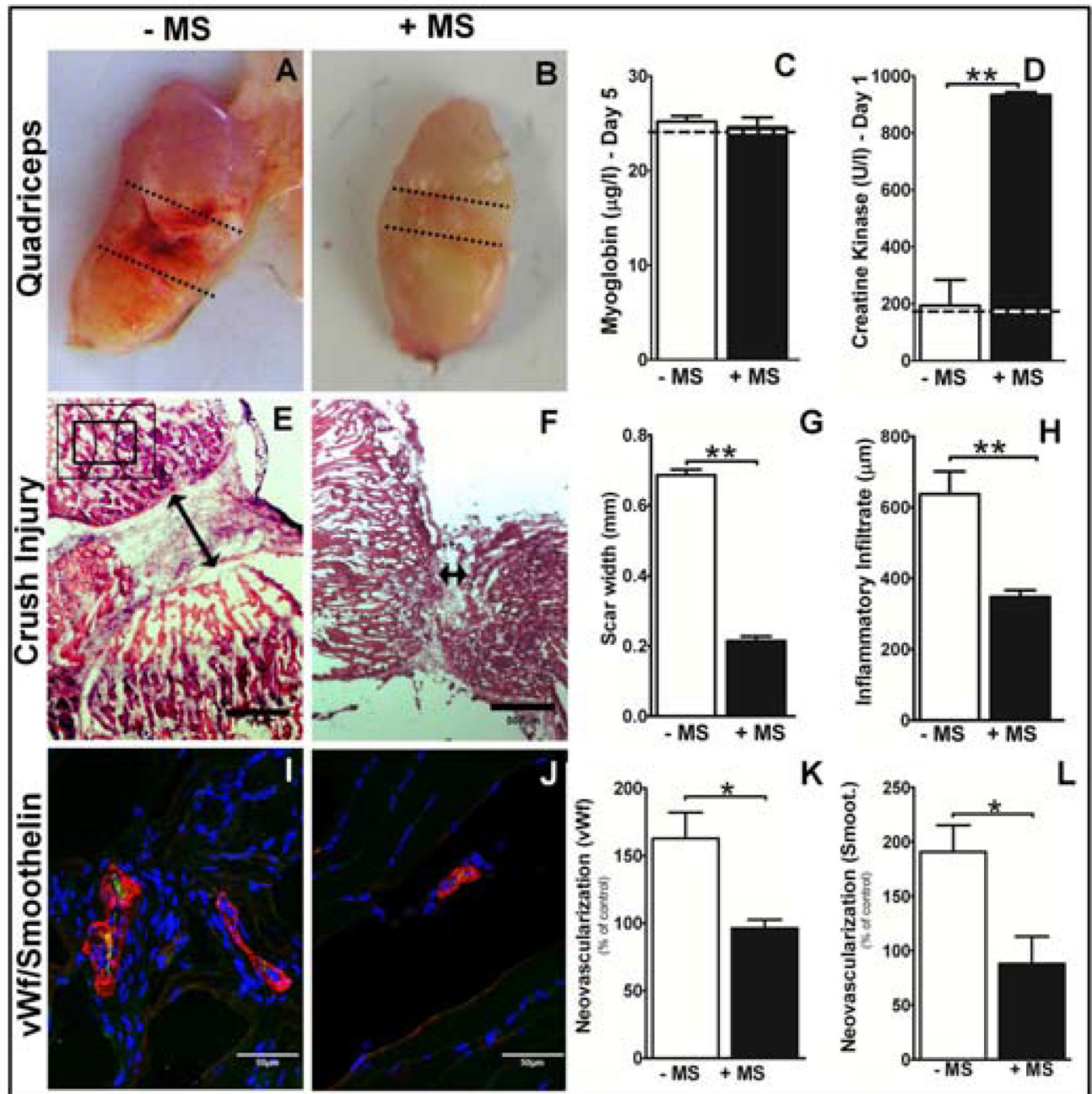


**Figure 1. MS causes no systemic damage, accelerates the regeneration process, and reduces scar width and inflammatory infiltrates.**

(A, B) The degree of injury to the quadriceps was reduced after MS treatment. (C) The levels of systemic myoglobin after MS stimulation were comparable with normal parameters. (D) Conversely, the systemic values of creatine kinase increased up to 5-fold. Dashed lines indicate normal values. (E, F, G) Hematoxylin and eosin-stained sections demonstrated that the crush injury scar was significantly reduced after 5 days of MS treatment. (H) Simultaneously, the extension of the inflammatory infiltrate, as assessed by the presence of lymphocytes and macrophages on the interface of injury, was reduced to

half. (I, J) Staining with smoothelin/Cy3 (red), von Willebrand factor/FITC (green) and DAPI (blue) demonstrated a lower density of new vessels at day 5 in the MS-treated samples. (K, L) While the control samples still displayed at least a 150% higher number of micro vessels when compared to intact quadriceps, MS-treated samples demonstrated values similar to native tissue. +MS indicates magnetic stimulation treatment, whereas -MS represents the non-stimulated controls (\* $P < 0.05$ , \*\* $P < 0.001$ ).



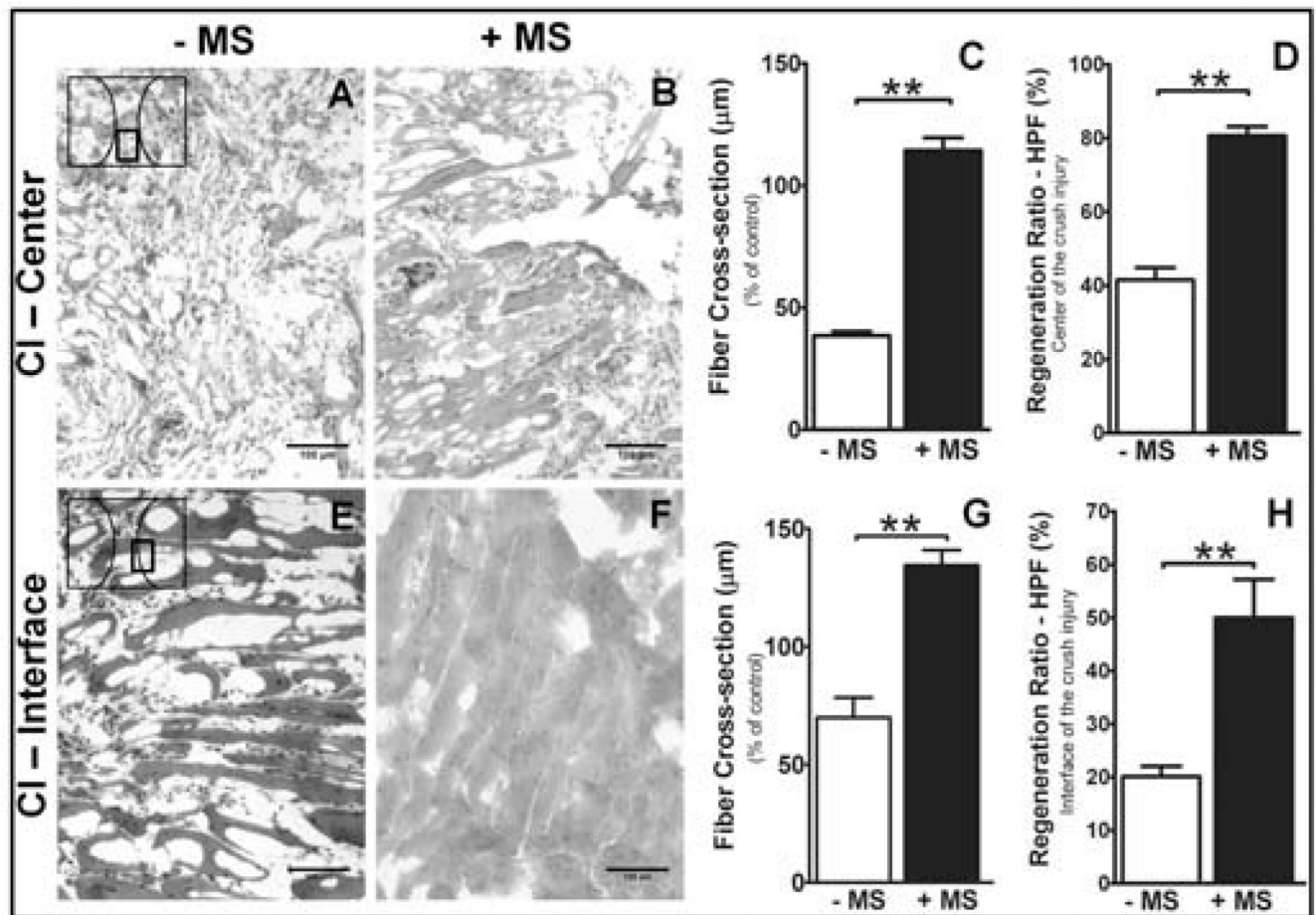


**Figure 2. MS reduces post-trauma muscle atrophy, boosts muscle turn-over, and induces hypertrophy of the injury interface.**

Muscle fiber cross-section measurements were performed in study animals after muscle crush with or without MS within the central zone of the injury and at the border. The values were then normalized with muscle fiber cross-section of the control unscathed muscle and expressed as percentage of it. The isolated effect of MS on the injury center (A-D) and on the interface (E-H) was analyzed. (A, B, C) In the center of the injury site, MS induced hypertrophy and doubled the cross-sectional diameter of the fibers. (D) This effect was associated with a remarkable increase in the regeneration ratio, as represented by muscle fibers with central nuclei. (E, F) Similarly, in the injury interface, the inflammatory infiltrate was reduced, and (G) the fiber cross-sections were again hypertrophic, with fiber cross-sections that were approximately 40% larger than in control and MS-untrained quadriceps. (H) The regeneration ratio, as assessed by the percentage of myofibers with central nuclei, was almost 3 times higher in stimulated samples. +MS indicates the presence of magnetic stimulation treatment, whereas -MS represents the unstimulated controls (\*\* $P < 0.001$ )

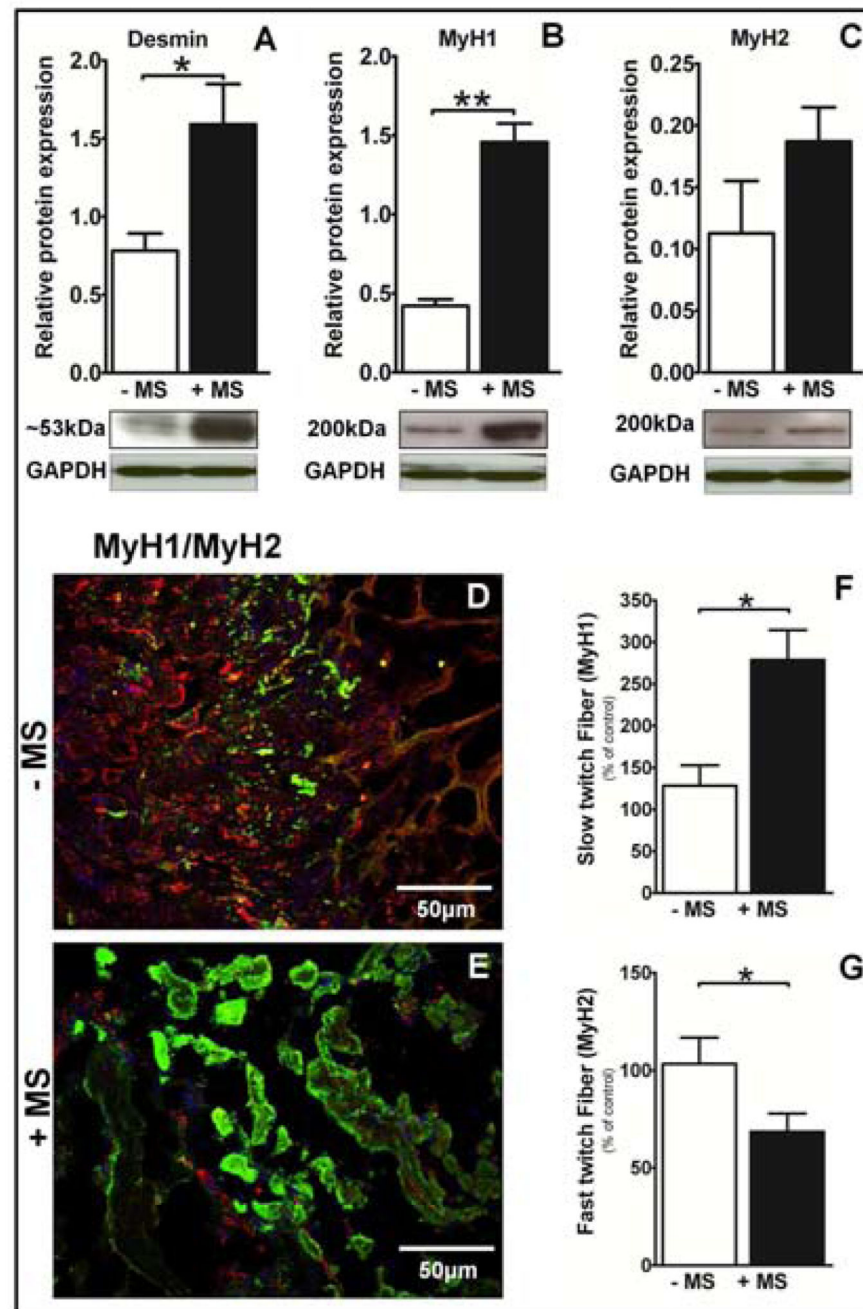


**Figure 3. MS induces a muscle type switch to slow-twitch fibers**

After crush injury and MS treatment, the quadriceps was retrieved and analyzed by western blot or histology. We found that the expression of muscle proteins was increased after MS treatment. (A) Desmin nearly doubled its expression levels, and (B) a specific increase in MyH type 1 could be detected. (C) No significant difference in MyH type 2 was found by WB. (D, E, F) Staining was performed with anti-myosin-heavy-chain-slowtwitch/FITC-anti-mouse-IgM (green), anti-myosin-heavy-chain-fast-twitch/Cy3-antimouse-IgG (red), and DAPI (blue). When compared with intact control quadriceps, no fiber type change was

found in injured muscle without MS stimulation. (E) On the other hand, a shift to type 1 fibers was verified in MS-treated samples. (F) MyH type 1 expression was up to 3-fold higher in MS-treated samples than in native muscle. (G) As expected, a relative decrease in MyH type 2 was detected. +MS indicates magnetic stimulation treatment, whereas -MS represents the unstimulated controls (\* $P < 0.05$ , \*\* $P < 0.001$ )

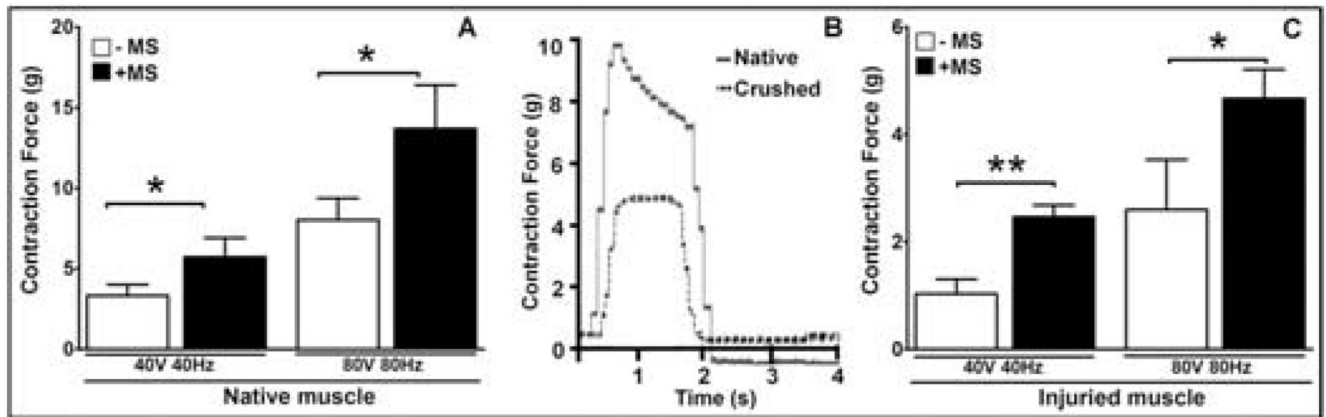


**Figure 4. MS improves muscle contractile strength of native control muscle tissue and aids in the recovery of muscle contractile strength after trauma**

After 5 days of magnetic stimulation, the muscles were retrieved and assessed. Organ bath of tibialis muscle strips was performed using 40-80V and 40-80Hz. (A) In native control muscle tissue, MS increased the contractile strength to 150% of non-stimulated samples. (B) Representative organ bath contractions at 40 V/40 Hz. The induced muscle crush injury was sufficient to reduce muscle contractile strength to approximately one-half (dashed line) of that of control muscles (continuous line). (C) MS treatment after injury significantly promoted the recovery of lost muscle strength after trauma. +MS indicates magnetic stimulation treatment, whereas -MS represents the non-stimulated controls (\* $P < 0.05$ , \*\* $P < 0.001$ ).

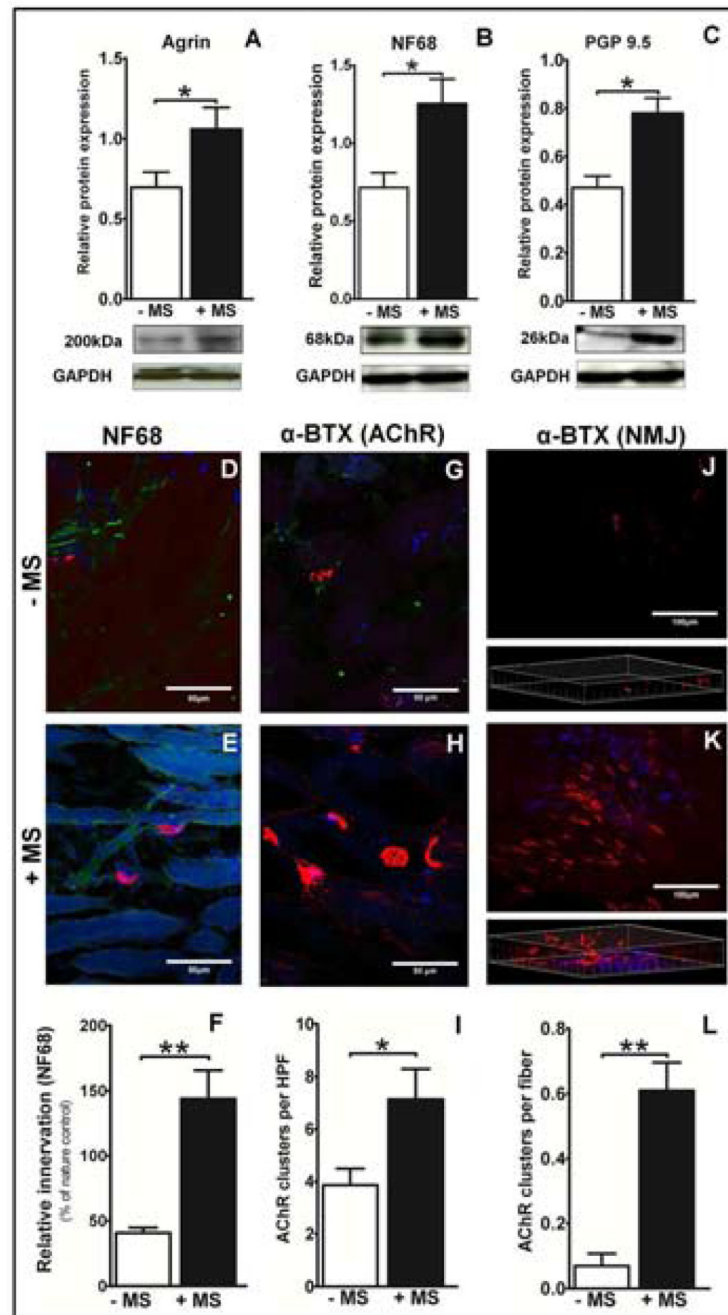


**Figure 5. MS intensifies muscle-nerve cross-talk, increases nerve ingrowth, and promotes AChR clustering.**

Analyses of the nerve component within the injured muscle were performed by WB and immunostaining. (A) Agrin expression was increased, (B, C) along with specific neurofilament 68 (NF68) and the PGP9.5-neuronal marker. (D, E) Immunostaining confirmed the WB results, demonstrating an increased number of nerves in the tissues after MS. Staining was performed with neurofilament 68/488-anti-mouse-IgG (green),  $\alpha$ -BTX (red), and DAPI (blue). (F) Surprisingly, the amount of nerves detected after MS was approximately 50% higher compared to normal tissue. (G, H, I) NMJ staining of

acetylcholine receptors (AChR) with  $\alpha$ -bungarotoxin (red) demonstrated that they were more clustered and had a significantly higher density after MS. (J, K) Analysis of single fibers isolated from the entire injury area after collagenase digestion demonstrated the total ratio of AChR cluster per muscle fiber. (L) The total number of clusters per fiber was 4-fold higher in MS-treated samples, demonstrating the positive effect of MS in reorganizing the neuromuscular junction after trauma. +MS indicates magnetic stimulation treatment, whereas -MS represents non-stimulated controls (\* $P<0.05$ , \*\* $P<0.001$ )